Published in final edited form as:
FEBS Lett. 2013 December 11; 587(24): 3973–3978. doi:10.1016/j.febslet.2013.10.032.

Differential Calmodulin-Modulatory and Electron Transfer Properties of Neuronal Nitric Oxide Synthase Mu Compared to the Alpha Variant

Satya P. Panda[1,4], **Wenbing Li**[2,4], **Priya Venkatakrishnan**[1], **Li Chen**[2], **Andrei V. Astashkin**[3], **Bettie Sue S. Masters**[1], **Changjian Feng**[2], and **Linda J. Roman**[1]

[1]Department of Biochemistry, University of Texas Health Science Center in San Antonio, San Antonio, TX 78229

[2]Department of Pharmaceutical Sciences, College of Pharmacy, University of New Mexico, Albuquerque, NM 87131

[3]Department of Chemistry and Biochemistry, University of Arizona, Tucson, AZ 85721

Abstract

Neuronal nitric oxide synthase μ (nNOSμ) contains 34 additional residues in an autoregulatory element compared to nNOSα. Cytochrome c and flavin reductions in the absence of calmodulin (CaM) were faster in nNOSμ than nNOSα, while rates in the presence of CaM were smaller. The magnitude of stimulation by CaM is thus notably lower in nNOSμ. No difference in NO production was observed, while electron transfer between the FMN and heme moieties and formation of an inhibitory ferrous-nitrosyl complex were slower in nNOSμ. Thus, the insert affects electron transfer rates, modulation of electron flow by CaM, and heme-nitrosyl complex formation.

Keywords

neuronal nitric oxide synthase; calmodulin; electron transfer; reductase; flavoproteins; heme

Nitric oxide synthases (NOSs) are heme- and flavin-containing enzymes that catalyze the synthesis of nitric oxide (NO) from L-arginine (L-Arg). There are three isoforms encoded by different genes, neuronal (nNOS), endothelial (eNOS), and inducible (iNOS). NO has been implicated in neurotransmission, hemodynamic control, and the immune response, depending on the isoform and the cell type in which it is being expressed (for review, see [1–3]). All NOSs are functional dimers, with each monomer containing an N-terminal oxygenase domain followed by a reductase domain containing at least two regulatory elements – the autoregulatory region (AR), a ~40 residue sequence in the FMN-binding subdomain [4–7] and the C-terminal tail region (CT) [8,9]. These oxygenase and reductase

To whom correspondence should be addressed: Linda J. Roman, PhD, Department of Biochemistry, University of Texas Health Science Center in San Antonio, 7703 Floyd Curl Dr., San Antonio, TX 78229, USA, Tel.: (210) 567-6979, Fax: (210) 567-6984, roman@uthscsa.edu.
[4]Contributed equally to this manuscript.

domains are connected by a CaM-binding site, to which CaM must be bound for electron transfer into the heme. Roman and Masters [10] proposed a model of NOS regulation in which the AR, in combination with the CT, stabilizes either a closed or an open form of the enzyme, depending on the binding of $NADP^+$/NADPH or CaM, which allows electron transfer between the FAD and FMN or between the FMN and the heme, respectively.

All NOS isoforms are expressed to some extent in mammalian skeletal muscle. In addition to nNOSα, skeletal muscle contains an alternatively spliced nNOS isoform, nNOSμ, which contains 34 additional amino acids within the AR [11]. The physiological role of either variant of nNOS in skeletal muscle is unclear, but in nNOS knockout (KN1) mice, skeletal muscle bulk and titanic force production were decreased, and muscles exhibited increased susceptibility to contraction-induced fatigue [12,13], implicating nNOS as having a role in the maintenance and function of muscle.

Despite the 34-residue difference, initial reports indicated that nNOSμ and nNOSα shared similar spectral properties, substrate and CaM binding values, and NO synthesis activity [11,14]. In the present work, we probed deeper into biochemical differences between these two proteins, demonstrating that the insertion affects CaM modulation of electron transfer of nNOSμ relative to nNOSα, and also alters the formation of the heme nitrosyl adduct formed during NO synthesis. Moreover, detailed FMN–heme interdomain electron transfer (IET) kinetics studies suggested differences in the FMN domain conformational equilibrium between the two proteins.

MATERIALS AND METHODS

Plasmids

The plasmid rat nNOSα pCW was as described [15]; that of nNOSμ pCW was made using the same protocol and oligonucleotides, with rat nNOSμ cDNA in pcDNA3 as template, kindly provided by David Bredt of Johnson and Johnson (San Diego). The plasmid encoding calmodulin, CaM ACMIP, was kindly provided by Anthony Persechini of the University of Missouri (Kansas City).

Protein Expression and Purification

Rat nNOSα and rat nNOSμ were expressed and purified as previously described [10], with a few modifications. After sonication, the lysate was applied to a 50ml DEAE Sepharose column (Sigma-Aldrich) equilibrated in 20mM Tris-HCl, pH 7.4, 100mM NaCl, 0.1mM EDTA, 0.1mM DTT, and 10% glycerol (Buffer B). Flow-through was loaded onto a 30ml 2’5’-ADP Sepharose affinity column equilibrated in Buffer B, washed with 300ml of Buffer B and eluted with 50ml Buffer B containing 500mM NaCl and 5mM 2’-AMP. Calmodulin was prepared as described [16].

Spectrophotometric Methods

CO difference spectra were obtained as described [15]. The molar protein concentrations for nNOSs were determined based on heme content via reduced CO difference spectra, where ε=100$mM^{-1}cm^{-1}$ for $\Delta A_{445\text{-}470}$. All spectral analyses were performed using a Shimadzu Model 2401PC UV/visible dual-beam spectrophotometer.

Activity Measurements

Nitric oxide formation and cytochrome *c* reduction were measured at 23°C as described [17,18], in pH 7.4 buffer containing 50mM Tris-HCl, 100mM NaCl, and 200μM $CaCl_2$. Rates of NO synthesis and cytochrome *c* reduction were determined using extinction coefficients of 60$mM^{-1}cm^{-1}$ at 401nm and 21$mM^{-1}cm^{-1}$ at 550nm, respectively.

Oxidation of NADPH was monitored at 340nm at 23° in pH 7.4 buffer containing 50mM Tris-HCl, 100mM NaCl, and 100μM NADPH, with or without added L-arginine and CaM, as indicated. The rate was determined using an extinction coefficient of 6.2$mM^{-1}cm^{-1}$ at 340nm for NADPH.

Stopped-flow Spectrophotometry

Stopped-flow reactions were performed aerobically under turnover conditions at 23°C, as described [9,19], using an Applied Photophysics SX.18MV diode array stopped-flow spectrophotometer. Reactions contained 1.5μM enzyme, 100μM NADPH, 10μM H_4B, and 100μM L-arginine in pH 7.4 buffer containing 50mM Tris-HCl, 100mM NaCl and, where indicated, 15μM CaM. Heme nitrosyl formation and flavin reduction were monitored at 436nm and 485nm, respectively.

Laser Flash Photolysis

CO photolysis experiments were conducted as described [3]. Briefly, a solution (~350μL) containing 20μM 5-deazariboflavin (dRF) and 5mM fresh semicarbazide in pH 7.6 buffer (40mM Bis-Tris propane, 400mM NaCl, 2mM L-Arg, 20μM H_4B, 1mM Ca^{2+} and 10% glycerol) was degassed in a laser photolysis cuvette by a mixture of 1:3 CO/Ar for 90min. Concentrated NOS was injected through a septum to the desired concentration, kept in ice, and further purged by passing the CO/Ar mixture over the surface for 60min. The protein was illuminated for an appropriate period to obtain a partially reduced form of [Fe(II)−CO] [$FMNH^{\bullet}$], then flashed with a 446nm laser excitation to trigger the FMN−heme IET, which was followed by the loss of absorbance of Fe(II) at 465 nm [20].

RESULTS

The absorption, EPR, and fluorescence spectra of the nNOSμ and nNOSα proteins are very similar (Figures S1 and S2 in Supporting Information), indicating that the insertion in nNOSμ likely does not perturb the protein environments of the heme and flavin moieties.

The presence of an additional 34 amino acids in nNOSμ in a known electron transfer regulatory region, the AR, might be expected to alter the rate of electron transfer through the reductase domain and/or into the oxygenase domain. Modulation of this activity by CaM, which both increases the electron transfer rate through the reductase domain and permits reduction of the heme, might also be altered. To examine this, NO synthesis activity, which requires electron transfer through the entire enzyme, and cytochrome c reduction, which probes electron transfer through the reductase domain only, were measured (Tables 1 **and** 2).

No difference in the rate of NO formation was observed between the variants (Table 1). Under optimal, fully coupled conditions, NO production requires 1.5 NADPH molecules per NO molecule formed. Deviation from this optimum indicates that reactive oxygen species are being formed at the expense of product (*i.e.*, uncoupling). NADPH oxidation was monitored during NO synthesis to assess coupling of this process to product NO formation. No difference in the NADPH oxidation rate was observed (Table 1), suggesting no difference in the degree of coupling between the variants.

The rate of cytochrome c reduction is dependent on the rate of electron flow through the reductase domain. In the absence of CaM, the rate of cytochrome c reduction is approximately 50% higher for nNOSμ over nNOSα, and is stimulated to a much lower extent by CaM in nNOSμ. However, the rate in the presence of CaM is 1.8-fold higher in nNOSα than nNOSμ (Table 2). Thus, electron transfer through the reductase domain of

nNOSμ is stimulated significantly less by CaM than that of nNOSα (3.5-fold *vs.* 9.7-fold for nNOSμ and nNOSα, respectively).

NO synthesis was measured at different NOS concentrations (25, 50, 75, and 100 nM) in the presence of increasing amounts of CaM (molar ratios of CaM:nNOS ranging from 0.25 to 5) to determine whether activation by CaM differs between nNOSα and nNOSμ. The data were analyzed as described [21], which is based on evaluation of tightly binding inhibitors [22]. The relationship between fractional velocity and the AC_{50} for CaM is given in equation 1:

$$y = v_{fmax}/(1+(AC_{50}/x)^n) \quad \text{Equation 1}$$

where, y is the fractional activity (rate/maximum rate),×is the concentration of CaM, v_{fmax} is the maximum fractional activity (when concentration of CaM approaches infinity), n is the Hill coefficient. The data for all nNOS enzyme concentrations were fit to equation 1 (Figure 1a,b) to derive AC_{50} values. The calculated AC_{50} values for nNOSα and nNOSμ were then plotted as a function of nNOS concentration. The estimated activation constant (K_{act}) for each enzyme is the ordinal intercept of the linear fit of this plot (Figure 1c). The K_{act} values were calculated to be 2.45 and 4.65 nM for nNOSα and nNOSμ, respectively. Thus, the 34-amino acid insertion in the AR appears to have little to no effect on CaM binding to nNOSμ, as measured indirectly by catalytic activity.

The rates of NO formation by nNOSα and nNOSμ at varying L-arginine concentration with different CaM concentrations were measured to determine the effect of CaM on substrate binding (Figure S3). The apparent K_m values were independent of CaM concentration (3.19 ± 1.2 μM and 3.68 ±1.95 μM (±std. dev.) for nNOSα and nNOSμ respectively), indicating that the interactions of both splice variants interaction with L-arginine are independent of CaM binding.

In addition to NO synthesis with L-Arg, NOSs oxidize NADPH in the absence of substrate, forming reactive oxygen species [23,24]. We compared rates of NADPH oxidation by the two variants in the absence of substrate L-Arg. The NADPH oxidation rates of nNOSα and nNOSμ in the absence of CaM are similar and very low (3±1 and 6±1 min^{-1}, respectively). In the presence of CaM, however, nNOSα oxidizes NADPH at approximately twice the rate of nNOSμ (490±10 and 260±4 min^{-1}, respectively), once again demonstrating that stimulation of activity by CaM is much lower for nNOSμ than nNOSα (45-fold vs. 154-fold, respectively).

Because stimulation by CaM affects electron transfer into the NOSs, as well as transfer between the two flavins and from FMN to the heme moiety, the rates of flavin reduction in the presence and absence of CaM were measured using stopped-flow spectrophotometry. This is a biphasic reaction, with a fast phase representing the initial input of electrons from NADPH [9,25] and a slow phase presumably reflecting comproportionation of the electrons between FAD and FMN. The fast rate of flavin reduction is equivalent for nNOSα and nNOSμ in the absence of CaM (Table 3, Figure S4 in Supporting Information). In the presence of CaM, however, the fast rate quadruples for nNOSα, but only doubles for nNOSμ, again showing that CaM stimulation of nNOSμ is half that of nNOSα. Similar behavior occurs in the slow phase of flavin reduction (Table 3).

As the interdomain electron transfer (IET) between the FMN and heme is essential for NO production at the catalytic heme site, IET kinetics of nNOSμ were measured using a laser flash photolysis approach [26,27]. As expected, CO dissociation by laser photolysis of the [Fe(II)−CO][$FMNH^{\bullet}$] form of CaM-bound nNOSμ results in a spectral “transition” (*i.e.*, a change in direction of absorbance changes over time) in the 460 nm traces of the nNOSμ protein. Figure S5 shows a typical kinetic trace of the nNOSμ protein at 21°C: a rapid decay

(with a rate constant k_1 of 33.4 ± 0.4 s^{-1}) below the pre-flash baseline, followed by a much slower recovery toward the baseline with a rate constant k_2 of 2.7 ± 0.1 s^{-1} (due to CO rebinding to Fe(II)). The rapid absorbance decay (Figure S5a) is due to net oxidation of heme in the following IET process, resulting in the loss of absorbance of Fe(II) at 460 nm [20,28,29]:

$$[\mathrm{Fe(II)}][\mathrm{FMNH^{\bullet}}] \rightleftharpoons [\mathrm{Fe(III)}][\mathrm{FMNhq}] \quad \text{Equation 2}$$

where FMNhq stands for the FMN hydroquinone species. No IET was observed in the absence of CaM (data not shown), confirming that IET in nNOSμ is activated upon CaM-binding, as in nNOSα. However, the FMN–heme IET rate constant for nNOSα at room temperature is 47 s^{-1} [27], about 40% larger than that of nNOSμ.

To compare activation parameters of IET in nNOSμ and nNOSα, IET rate constants k_{et} were determined over the temperature range 283–304K (Table S1 in Supporting Information). An appreciable increase in the IET rate constant was observed with increasing temperature. Importantly, the obtained rate constant of the rapid decay (Figure S5a) is independent of the signal amplitude in the range of temperature studied (data not shown), confirming an intraprotein IET process.

Viscosity studies indicated that the NOS FMN−heme IET process is conformationally gated [30]. The temperature dependence of k_{et} was thus analyzed by transition state theory using the Eyring equation:

$$\ln(k_{et}/T) = -\Delta H^{\ddagger}/RT + \Delta S^{\ddagger}/R + \ln(k_B/h) \quad \text{Equation 3}$$

where ΔH is activation enthalpy, ΔS is activation entropy, h is Planck's constant, k_B is the Boltzmann constant, and R is the gas constant. The parameters of the nNOSμ data fit to eq 2 (Figure 2) are listed in Table 4, along with those of the nNOSα protein. The obtained activation values are comparable to those of inter-flavin electron transfer in human cytochrome P450 reductase [31], which is homologous to NOS reductase domain. The nNOSα activation enthalpy value (37.9 ± 3.2 kJ/mol) is comparable to that of nNOSμ, while its activation entropy value (−82.2 ± 7.9 J/mol/K) is notably smaller (Table 4).

Approximately 80% of nNOSα has been estimated to be quickly converted to an inactive form due to ferrous-nitrosyl complex formation [32–34], functioning to down-regulate NO synthesis. To compare this behavior between the two nNOS variants, ferrous-nitrosyl complex formation was monitored by stopped-flow spectrophotometry. The kinetics of heme-nitrosyl formation are complex, involving several steps [34]. The resulting trace was best fit by a triple exponential; curve fits are shown in Figure S5 of the supporting information. The initial rate, *i.e.*, the formation of the ferrous-nitrosyl complex, of nNOSμ is almost half that of nNOSα (Table 3 and Figure 3), indicating that nNOSμ is inactivated at a much slower rate. In addition, the amplitude of the complex formation (Figure 3) is lower for nNOSμ, indicating that a smaller proportion is in this inactivated state.

DISCUSSION

The nNOS splice variant nNOSμ is found primarily in differentiated skeletal muscle and heart [11], while most other tissues express nNOSα. The expression of nNOSμ only in certain tissue types as well as the presence of the additional 34 amino acids in the auto-regulatory (AR) regions warrants a detailed mechanistic study of this variant in comparison to the much-studied variant, nNOSα. No major difference in the rate of NO production by nNOSμ vs. nNOSα was observed, corroborating prior results [14]. The rates of cytochrome

c and flavin reduction in the absence of CaM were faster in nNOSμ than nNOSα, while the rates in the presence of CaM were smaller in nNOSμ. The magnitude of stimulation of the rate by CaM is thus notably lower in nNOSμ. The activation of nNOSα and nNOSμ by CaM shows little or no difference as the Kact values were 2.45 and 4.65 nM, respectively, indicating that the 34 amino acid insert in nNOSμ doesn't appear to alter the apparent affinity of CaM for the enzyme.

The measured FMN-heme IET rate of nNOSα is also higher than in nNOSμ. Despite the differences in the rate of electron flow, the rates of NO production by nNOSα and nNOSμ are similar (Table 1); this may be explained by a difference in their rates of autoinhibition by NO (Figure 4) as all NOS isoforms are autoinhibited by NO to some degree due to the binding of NO to the heme to form a ferrous-nitrosyl complex [32,34]. The rate of ferrous nitrosyl complex formation is higher in nNOSα than in nNOSμ, and the percent difference between the variants is similar to that of the FMN–heme IET rates, indicating that the heme-NO complex formation is directly linked to the heme reduction rate. Previous studies of a nNOSα S1412D mutant also support this connection [35]. Thus it is likely that, at any given time under steady-state turnover conditions, more nNOSα exists in an inhibited state compared to nNOSμ, which may have physiological significance for skeletal muscle function.

The FMN–heme IET rate constant of nNOSα is about 40% larger than that of nNOSμ, and the activation entropy of nNOSα is notably smaller than nNOSμ (Table 4). Interestingly, the order of the IET rate constant (nNOSα > nNOSμ) correlates with the order of the magnitude of the activation entropy (Table 4). This can be explained by a conformational sampling model, in which sampling of a continuum of conformational states gives a range of transient donoracceptor complexes, only a subset of which are IET-competent [36–38]; this avoids the necessity for tight binding of the FMN domain to achieve efficient IET. During NOS catalysis, the FMN domain cycles between the interaction with the NADPH/FAD domain (to receive electrons) and the interaction with the heme-containing oxygenase domain (to deliver electrons to the heme) [39], favoring the interaction with the NADPH/FAD domain [40]. In the NOS holoenzyme, even in the presence of bound CaM, the dominant conformational state is the docked FAD/FMN state [41], which must undergo a transformation to an IET-active, docked FMN/heme conformation before the FMN–heme IET occurs. Interdomain FMN/heme interactions in the NOS enzymes are rather weak, and the docked IET complexes are short-lived [30,40]. The observed rate of heme reduction is thus limited by the relatively infrequent formation of the docked IET-competent complexes. The larger negative activation entropy of nNOSμ indicates that the FMN domain needs to search for the IET-active conformation among a larger number of conformations that are not IET-competent than the nNOSα protein, resulting in less frequent formation of the FMN/heme complex and slower subsequent IET.

How an insertion of 34 residues in a regulatory region of the reductase domain influences the rates of heme reduction and ferrous nitrosyl complex formation is unknown, but one possibility is that the insert affects the stabilities and thus the time spent in various conformational states. The transfer of electrons to the heme requires the FMN domain to shuttle between an input (closed) or electron-accepting state and an output (open) or electron-donating state [39]. It was proposed that the AR and CT regulatory elements interact in some manner to stabilize either the open or closed conformation, depending on whether CaM and/or NADPH/$NADP^+$ are bound [10]. Indeed, deletion of the AR regulatory element decreased the amount of enzyme present in the open conformation, implicating the AR as playing a role in the stability of the open complex [27]. Thus, the rate of electron transfer within the reductase domain and from the reductase to the oxygenase domain can be readily influenced by the dwell time in either a closed or open conformation.

The structural and functional aspects behind the differences in NADPH oxidation by the two variants in the absence of substrate L-Arg may have profound implications on downstream signaling mediated by NO and/or production of reactive oxygen species (ROS), both of which can be produced by NOSs [24]. Reactions between NO and various oxygen species form products such as peroxynitrite and nitrate, which also have downstream effects. The observed decrease in NADPH oxidation by nNOSμ might be of great physiological importance as nNOSμ is differentially expressed only in heart and skeletal muscle. It will be important to curb or minimize the possible oxidative stress caused by nNOSμ as its expression/activity is upregulated under exercise conditions [42]or by insulin stimulation [43]. Because these two nNOS isoforms have very similar catalytic properties *in vitro*, the sequence differences between them may also allow for differential regulation through protein/protein interactions and/or differential subcellular localization *in vivo*.

In conclusion, detailed biochemical analysis of nNOSμ and its comparison with nNOSα demonstrates that the presence of 34 additional residues in the AR affects electron flow through the enzyme, the enzyme's response to CaM, and the formation of an inhibitory heme-nitrosyl complex. In addition, these studies suggested differences in the conformational equilibrium of the FMN domain, an important determinant of electron flux in NOS.

Supplementary Material

Refer to Web version on PubMed Central for supplementary material.

Acknowledgments

The authors thank Dr. Kenneth M. Roberts, Dept. of Biochemistry, UTHSCSA, for his help in acquiring some of the stopped-flow data. This work was supported by NIH GM052419 to LJR and BSM, NIH GM081811 to CF, NSF CHE-1150644 to CF, and AHA Grant-in-Aid 12GRNT11780019 to CF. This project was also supported by grants from the National Center for Research Resources (5P20RR016480-12) and the National Institute of General Medical Sciences (8 P20 GM103451-12). BSM is the Robert A. Welch Distinguished Chair in Chemistry (AQ0012).

Abbreviations

NO	nitric oxide
NOS	nitric oxide synthase
nNOS	neuronal NOS
CaM	calmodulin
IET	interdomain electron transfer
L-Arg	L-Arginine
H_4B	tetrahydrobiopterin
AR	autoregulatory region
CT	C-terminal tail region

REFERENCES

1. Roman LJ, Martasek P, Masters BS. Intrinsic and extrinsic modulation of nitric oxide synthase activity. Chem Rev. 2002; 102:1179–1190. [PubMed: 11942792]

2. Stuehr DJ, Tejero J, Haque MM. Structural and mechanistic aspects of flavoproteins: electron transfer through the nitric oxide synthase flavoprotein domain. FEBS J. 2009; 276:3959–3974. [PubMed: 19583767]
3. Feng C. Mechanism of Nitric Oxide Synthase Regulation: Electron Transfer and Interdomain Interactions. Coord Chem Rev. 2012; 256:393–411. [PubMed: 22523434]
4. Salerno JC, Harris DE, Irizarry K, Patel B, Morales AJ, Smith SM, Martásek P, Roman LJ, Masters BSS, Jones CL, Weissman BA, Lane P, Liu Q, Gross SS. An autoinhibitory control element defines calcium-regulated isoforms of nitric oxide synthase. J Biol Chem. 1997; 272:29769–29777. [PubMed: 9368047]
5. Daff S, Sagami I, Shimizu T. The 42-amino acid insert in the FMN domain of neuronal nitric-oxide synthase exerts control over Ca(2+)/calmodulin-dependent electron transfer. J Biol Chem. 1999; 274:30589–30595. [PubMed: 10521442]
6. Lane P, Gross SS. The autoinhibitory control element and calmodulin conspire to provide physiological modulation of endothelial and neuronal nitric oxide synthase activity. Acta Physiol Scand. 2000; 168:53–63. [PubMed: 10691780]
7. Montgomery HJ, Romanov V, Guillemette JG. Removal of a putative inhibitory element reduces the calcium-dependent calmodulin activation of neuronal nitric-oxide synthase. J Biol Chem. 2000; 275:5052–5058. [PubMed: 10671547]
8. Roman LJ, Miller RT, de La Garza MA, Kim JJ, Masters BS. The C terminus of mouse macrophage inducible nitric-oxide synthase attenuates electron flow through the flavin domain. J Biol Chem. 2000; 275:21914–21919. [PubMed: 10781602]
9. Roman LJ, Martasek P, Miller RT, Harris DE, de La Garza MA, Shea TM, Kim JJ, Masters BS. The C termini of constitutive nitric-oxide synthases control electron flow through the flavin and heme domains and affect modulation by calmodulin. J Biol Chem. 2000; 275:29225–29232. [PubMed: 10871625]
10. Roman LJ, Masters BSS. Electron transfer by neuronal nitric-oxide synthase is regulated by concerted interaction of calmodulin and two intrinsic regulatory elements. J. Biol. Chem. 2006; 281:23111–23118. [PubMed: 16782703]
11. Silvagno F, Xia H, Bredt DS. Neuronal nitric-oxide synthase-mu, an alternatively spliced isoform expressed in differentiated skeletal muscle. Journal of Biological Chemistry. 1996; 271:11204. [PubMed: 8626668]
12. Percival JM, Anderson KN, Gregorevic P, Chamberlain JS, Froehner SC. Functional deficits in nNOSmu-deficient skeletal muscle: myopathy in nNOS knockout mice. PLoS One. 2008; 3:e3387. [PubMed: 18852886]
13. Wehling-Henricks M, Oltmann M, Rinaldi C, Myung KH, Tidball JG. Loss of positive allosteric interactions between neuronal nitric oxide synthase and phosphofructokinase contributes to defects in glycolysis and increased fatigability in muscular dystrophy. Hum Mol Genet. 2009; 18:3439–3451. [PubMed: 19542095]
14. Lainé R, Ortiz de Montellano PR. Neuronal nitric oxide synthase isoforms alpha and mu are closely related calpain-sensitive proteins. Mol Pharmacol. 1998; 54:305–312. [PubMed: 9687572]
15. Roman LJ, Sheta EA, Martásek P, Gross SS, Liu Q, Masters BSS. High-level expression of functional rat neuronal nitric oxide synthase in Escherichia coli. Proc Natl Acad Sci U S A. 1995; 92:8428–8432. [PubMed: 7545302]
16. Zhang M, Vogel HJ. Characterization of the calmodulin-binding domain of rat cerebellar nitric oxide synthase. J Biol Chem. 1994; 269:981–985. [PubMed: 7507114]
17. Hevel JM, Marletta MA. Nitric-oxide synthase assays. Methods Enzymol. 1994; 233:250–258. [PubMed: 7516999]
18. Martásek P, Miller RT, Roman LJ, Shea T, Masters BS. Assay of isoforms of Escherichia coli-expressed nitric oxide synthase. Methods Enzymol. 1999; 301:70–78. [PubMed: 9919555]
19. Miller RT, Martásek P, Omura T, Masters BSS. Rapid kinetic studies of electron transfer in the three isoforms of nitric oxide synthase. Biochem Biophys Res Commun. 1999; 265:184–188. [PubMed: 10548511]

20. Feng C, Dupont AL, Nahm NJ, Spratt DE, Hazzard JT, Weinberg JB, Guillemette JG, Tollin G, Ghosh DK. Intraprotein electron transfer in inducible nitric oxide synthase holoenzyme. JBIC Journal of Biological Inorganic Chemistry. 2009; 14:133–142.
21. Montgomery HJ, Bartlett R, Perdicakis B, Jervis E, Squier TC, Guillemette JG. Activation of constitutive nitric oxide synthases by oxidized calmodulin mutants. Biochemistry. 2003; 42:7759–7768. [PubMed: 12820885]
22. Copeland, RA. Enzymes: a practical introduction to structure, mechanism, and data analysis. New York: Wiley; 2000.
23. Pou S, Pou WS, Bredt DS, Snyder SH, Rosen GM. Generation of superoxide by purified brain nitric oxide synthase. J Biol Chem. 1992; 267:24173–24176. [PubMed: 1280257]
24. Miller RT, Martasek P, Roman LJ, Nishimura JS, Masters BS. Involvement of the reductase domain of neuronal nitric oxide synthase in superoxide anion production. Biochemistry. 1997; 36:15277–15284. [PubMed: 9398256]
25. Matsuda H, Iyanagi T. Calmodulin activates intramolecular electron transfer between the two flavins of neuronal nitric oxide synthase flavin domain. Biochim Biophys Acta. 1999; 1473:345–355. [PubMed: 10594372]
26. Feng C, Tollin G, Hazzard JT, Nahm NJ, Guillemette JG, Salerno JC, Ghosh DK. Direct Measurement by Laser Flash Photolysis of Intraprotein Electron Transfer in a Rat Neuronal Nitric Oxide Synthase. J. Am. Chem. Soc. 2007; 129:5621–5629. [PubMed: 17425311]
27. Feng C, Roman LJ, Hazzard JT, Ghosh DK, Tollin G, Masters BSS. Deletion of the autoregulatory insert modulates intraprotein electron transfer in rat neuronal nitric oxide synthase. FEBS Letters. 2008; 582:2768–2772. [PubMed: 18625229]
28. Li W, Fan W, Chen L, Elmore BO, Piazza M, Guillemette JG, Feng C. Role of an isoform-specific serine residue in FMN-heme electron transfer in inducible nitric oxide synthase. J Biol Inorg Chem. 2012; 17:675–685. [PubMed: 22407542]
29. Feng C, Tollin G, Holliday MA, Thomas C, Salerno JC, Enemark JH, Ghosh DK. Intraprotein Electron Transfer in a Two-Domain Construct of Neuronal Nitric Oxide Synthase: The Output State in Nitric Oxide Formation. Biochemistry. 2006; 45:6354–6362. [PubMed: 16700546]
30. Li W, Fan W, Elmore BO, Feng C. Effect of solution viscosity on intraprotein electron transfer between the FMN and heme domains in inducible nitric oxide synthase. FEBS Lett. 2011; 585:2622–2626. [PubMed: 21803041]
31. Hay S, Brenner S, Khara B, Quinn AM, Rigby SE, Scrutton NS. Nature of the energy landscape for gated electron transfer in a dynamic redox protein. Journal of the American Chemical Society. 2010; 132:9738–9745. [PubMed: 20572660]
32. Griscavage JM, Fukuto JM, Komori Y, Ignarro LJ. Nitric oxide inhibits neuronal nitric oxide synthase by interacting with the heme prosthetic group. Role of tetrahydrobiopterin in modulating the inhibitory action of nitric oxide. J Biol Chem. 1994; 269:21644–21649. [PubMed: 7520440]
33. Wang J, Rousseau DL, Abu-Soud HM, Stuehr DJ. Heme coordination of NO in NO synthase. Proc Natl Acad Sci U S A. 1994; 91:10512–10516. [PubMed: 7524095]
34. Abu-Soud HM, Wang J, Rousseau DL, Fukuto JM, Ignarro LJ, Stuehr DJ. Neuronal nitric oxide synthase self-inactivates by forming a ferrous- nitrosyl complex during aerobic catalysis. J Biol Chem. 1995; 270:22997–23006. [PubMed: 7559438]
35. Adak S, Santolini J, Tikunova S, Wang Q, Johnson JD, Stuehr DJ. Neuronal nitric-oxide synthase mutant (Ser-1412 --> Asp) demonstrates surprising connections between heme reduction, NO complex formation, and catalysis. J Biol Chem. 2001; 276:1244–1252. [PubMed: 11038355]
36. Leys D, Scrutton NS. Electrical circuitry in biology: emerging principles from protein structure. Curr Opin Struct Biol. 2004; 14:642–647. [PubMed: 15582386]
37. Salerno JC, Ray K, Poulos T, Li H, Ghosh DK. Calmodulin activates neuronal nitric oxide synthase by enabling transitions between conformational states. FEBS Lett. 2013; 587:44–47. [PubMed: 23159936]
38. Li W, Chen L, Lu C, Elmore BO, Astashkin AV, Rousseau DL, Yeh SR, Feng C. Regulatory Role of Glu546 in Flavin Mononucleotide - Heme Electron Transfer in Human Inducible Nitric Oxide Synthase. Inorg Chem. 2013; 52:4795–4801. [PubMed: 23570607]

39. Ghosh DK, Salerno JC. Nitric oxide synthases: domain structure and alignment in enzyme function and control. Front Biosci. 2003; 8:d193–d209. [PubMed: 12456347]

40. Ilagan RP, Tejero J, Aulak KS, Ray SS, Hemann C, Wang ZQ, Gangoda M, Zweier JL, Stuehr DJ. Regulation of FMN subdomain interactions and function in neuronal nitric oxide synthase. Biochemistry. 2009; 48:3864–3876. [PubMed: 19290671]

41. Ghosh DK, Ray K, Rogers AJ, Nahm NJ, Salerno JC. FMN fluorescence in inducible NOS constructs reveals a series of conformational states involved in the reductase catalytic cycle. FEBS J. 2012; 279:1306–1317. [PubMed: 22325715]

42. McConell GK, Bradley SJ, Stephens TJ, Canny BJ, Kingwell BA, Lee-Young RS. Skeletal muscle nNOS mu protein content is increased by exercise training in humans. Am J Physiol Regul Integr Comp Physiol. 2007; 293:R821–R828. [PubMed: 17459909]

43. Hinchee-Rodriguez K, Garg N, Venkatakrishnan P, Roman MG, Adamo ML, Masters BS, Roman LJ. Neuronal nitric oxide synthase is phosphorylated in response to insulin stimulation in skeletal muscle. Biochem Biophys Res Commun. 2013; 435:501–505. [PubMed: 23680665]

Highlights

- nNOSμ contains 34 extra residues, compared to nNOSα, in a regulatory element.
- Electron transfer, heme nitrosyl formation, and CaM-stimulation are lower in nNOSμ.
- nNOSμ activity is adapted specifically for the skeletal muscle environment.

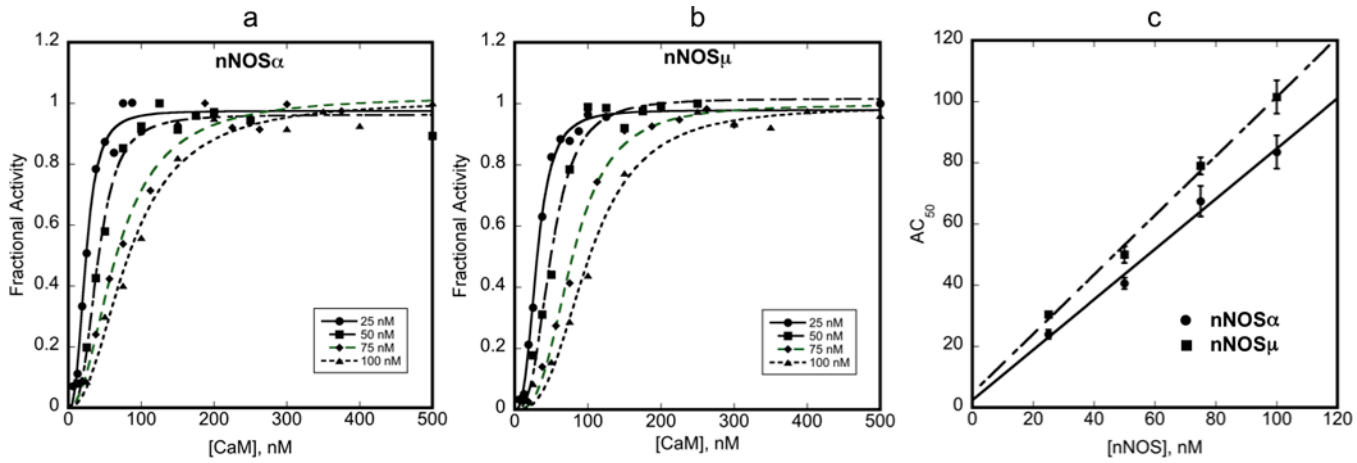

Figure 1.

Determination of CaM activation constant (Kact) of nNOSμ and nNOSμ. The rates of NO production by nNOSα and nNOSμ were measured at different enzyme concentrations (25 nM, 50 nM, 75 nM and 100 nM) with varying CaM concentrations (6.25 nM – 500 nM). The AC_{50} values were calculated for each nNOS concentration for both nNOSα (a) and nNOSμ (b) using equation 1 (R>0.99 for all fits). AC_{50} values were plotted against nNOS concentration (c) to determine K_{act} for CaM. R=0.9949 and 0.9975 for the linear fits of nNOSα and nNOSμ data, respectively.

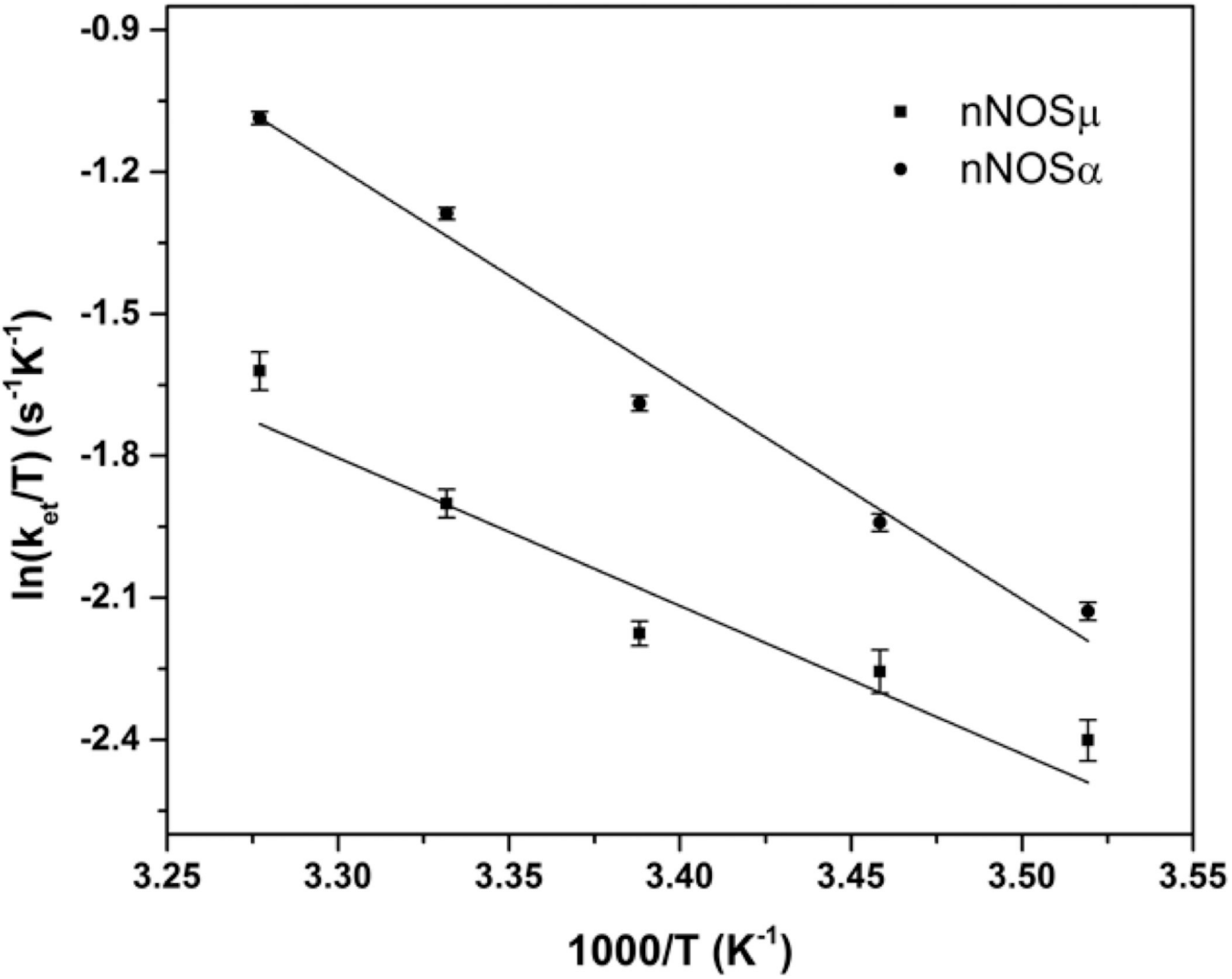

Figure 2.

Eyring plots showing the temperature dependence of k_{et} for nNOSμ (squares) and nNOSα (circles). The obtained Δ*H* and Δ*S* values are listed in Table 4.

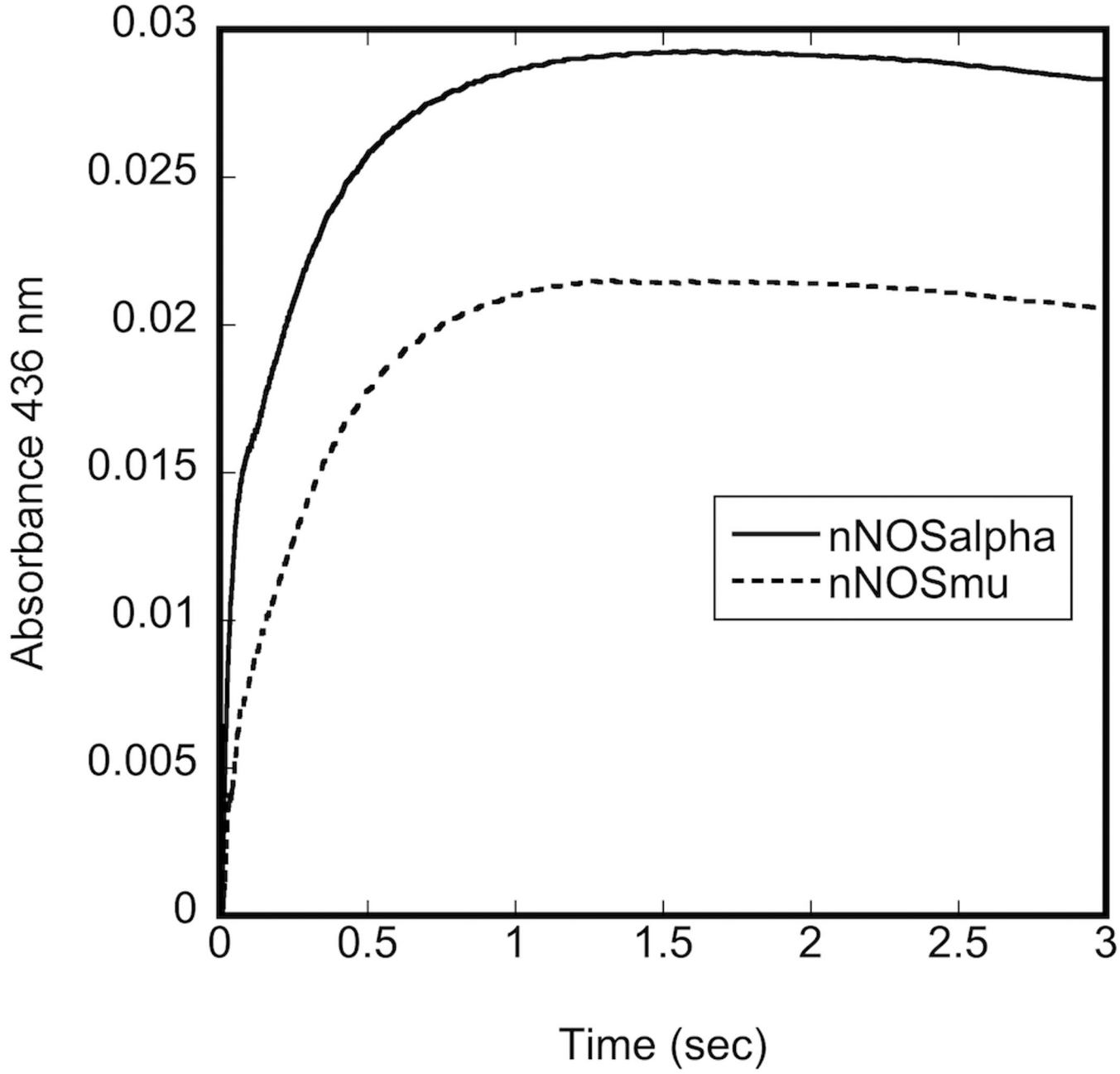

Figure 3.

Rate of ferrous nitrosyl complex formation monitored as a change in absorbance at 436nm under turnover conditions using a stopped-flow apparatus. Conditions are as described in Methods and Materials. Solid line: nNOSα, dashed line: nNOSμ. Traces shown represent an average of 3–5 experiments.

Table 1

Rates of NO synthesis and NADPH oxidation in the presence of substrate

Conditions are as described in Methods and Materials. Final nNOS and CaM concentrations are 0.1 and 1μM, respectively. Rates reported are the average of at least 3 reactions ± SEM.

	NO synthesis (min^{-1})	NADPH oxidation (min^{-1})	Efficiency of coupling (NADPH/NO)
nNOSα			
(+) CaM	53.4 ± 5.0	113.8 ± 4.5	2.1
nNOSμ			
(+) CaM	53.7 ± 1.1	125.1 ± 13.2	2.3

Table 2

Rates of cytochrome c reduction in the absence and presence of CaM

Conditions are as described in Methods and Materials. Final nNOS and CaM concentrations are 1 and 50nM, respectively. Rates reported are the average of at least 3 reactions ± SEM.

	Cytochrome c reduction (min^{-1})	CaM Stimulation
nNOSα		
(−) CaM	852 ± 58	9.7x
(+) CaM	8290 ± 54	
nNOSμ		
(−) CaM	1280 ± 45	3.5x
(+) CaM	4503 ± 380	

Table 3

Rapid kinetics measurements of flavin reduction and ferrous-nitrosyl complex formation

Conditions are as described in Methods and Materials. Rates reported are the derived from 3–5 reactions averaged together and fit to a double exponential for flavin reduction and a single exponential for heme nitrosyl formation.

	Flavin reduction (fast) (sec^{-1})	Flavin reduction (slow) (sec^{-1})	CaM Stimulation (fast/slow)	Heme nitrosyl formation (sec^{-1})
nNOSα				
(−) CaM	118.98 ± 2.52	7.90 ± 0.15	3.4x/3.5x	nd*
(+) CaM	401 ± 14.79	27.82 ± 0.42		41.85 ± 1.11
nNOSμ				
(−) CaM	124.72 ± 2.69	10.67 ± 0.14	1.5x/1.7x	nd*
(+) CaM	192.24 ± 4.57	18.26 ± 0.25		24.46 ± 1.4

* not detectable

Table 4

Eyring parameters from temperature dependence analysis of observed rate constants for the FMN–heme IET in nNOS holoenzymes, along with the FMN-heme IET rates k_{et} at room temperature

	ΔH (kJ/mol)	ΔS (J/mol/K)	k_{et} (s^{-1})
rat nNOSμ holoenzyme	25.7 ± 4.5	−127.2 ± 28.2	33.4 ± 0.4
rat nNOSα holoenzyme	37.9 ± 3.2	−82.2 ± 7.9	47 ± 4 [a]

[a] Data taken from ref. [27].